Behavioral/Systems/Cognitive

A Map of Angular Tuning Preference in Thalamic Barreloids

Elena Timofeeva, Chantal Mérette, Claudia Émond, Philippe Lavallée, and Martin Deschênes
Centre de Recherche Université Laval-Robert Giffard, Québec G1J 2G3, Canada

A double-labeling protocol was used to determine how cells with different angular preferences to whisker motion distribute across the dimensions of a barreloid in the ventral posterior medial nucleus of the rat thalamus. Individual barreloids were labeled retrogradely by injecting Fluoro-Gold in identified barrel columns, and single relay cells ($n = 30$) pertaining to the labeled barreloids were stained juxtacellularly with Neurobiotin after determination of their angular tuning preference to controlled whisker deflection. Results show that cells with like angular preference are clustered within the barreloids. Those best tuned to forward and upward directions are located principally in the dorsal sector of the barreloid, whereas those best tuned to backward and downward motion are located principally in the central and ventral sectors, respectively. The relationship between cell location and angular preference was assessed by regression, cluster, and discriminant analysis. Together, these tests indicate that barreloids contain a map of shifting angular preference that transposes along the length of a barreloid directional property imposed at the periphery by the circumferential distribution of receptors around the vibrissa follicles.

Key words: **barrel; somatosensory; thalamus; vibrissa; somatotopy; trigeminal**

Introduction

In all sensory systems, central relay stations contain topographic maps derived from the fine-grained innervation of sensory epithelia, or maps of higher integration level, termed "computational maps," in which the tuning of neighboring neurons for a particular stimulus parameter value varies systematically. Numerous computational maps have been discovered, particularly in the visual and auditory systems (for review, see Knudsen et al., 1987).

In the vibrissal system of rodents, the array of sinus hairs on the mystacial pad is represented centrally by homologous arrangements of cellular aggregates. In the ventral posterior medial (VPM) nucleus of the thalamus, whisker-related aggregates are called barreloids (Van der Loos, 1976), and each barreloid pairs with a corresponding module, called a barrel, in the primary somatosensory cortex (Woolsey and Van der Loos, 1970). In rats, barreloids representing the large caudal vibrissas have an elongated, pepper-like shape, and each contains ~200 cells that best respond to the motion of the same vibrissa (Land et al., 1995; Varga et al., 2002). So, the question naturally arises of what is represented across the dimensions of a barreloid. Confocal reconstructions of individual peripheral axons that innervate the vibrissas have shown that the terminal branches of single fibers in contact with Merkel endings are restricted along one margin of the follicle (Ebara et al., 2002), which suggests that the location of receptors around the follicle is what confers directional selectivity on primary afferent responses (Zucker and Welker, 1969; Gibson and Welker, 1983; Lichtenstein et al., 1990; Shoykhet et al., 2000). Thus, if a topographic or computational map is present within vibrissa-related modules in the brain, it likely translates into a map related to angular preference to whisker motion. Previous studies of whisker-responsive units in the principal trigeminal nucleus (PR5) and VPM have shown that directional sensitivity is a well conserved feature in the whisker–barrel pathway (Ito, 1988; Simons and Carvell, 1989; Lee et al., 1994; Brecht and Sakmann, 2002; Minnery and Simons, 2003; Minnery et al., 2003). Yet, little evidence has been provided for the existence of an angular preference map at any level (but see Temereanca and Simons, 2003). In the present study, we directly addressed this issue by means of a double-labeling protocol to determine how the location of a cell within a barreloid relates to the angular preference of its responses.

Received Aug. 21, 2003; revised Sept. 22, 2003; accepted Oct. 2, 2003.

This work was supported by Canadian Institutes for Health Research Grant MT-5877 (M.D.) and a Natural Sciences and Engineering Research Council postdoctoral fellowship (E.T.). We thank Drs. D. J. Simons and C. I. Moore for critical reading of a previous version of this manuscript.

Correspondence should be addressed to Dr. Martin Deschênes, Centre de Recherche Université Laval-Robert Giffard, 2601 de la Canardière, Québec City G1J 2G3, Canada. E-mail: martin.deschenes@crulrg.ulaval.ca.

 0270-6474/03/2310717-07$15.00/0

Materials and Methods

Animal preparation and recordings. Experiments were performed in 40 female and 5 male rats (250–300 gm; Sprague Dawley) in accordance with federally prescribed animal care and use guidelines. First, rats were anesthetized with a mixture of ketamine (75 mg/kg) plus xylazine (5 mg/kg), and a barrel column in the right hemisphere, usually in the C or D rows, was located by recording unit responses to manual whisker deflection. Then, a micropipette (tip diameter, ~6 μm) containing Fluoro-Gold (FG; 2% in 0.1 M cacodylate buffer, pH 7.0; Fluorochrome Inc., Denver, CO) was lowered in layer 4 (depth, 740 μm) of the identified barrel column. The tracer was ejected with positive current pulses (duration, 2 sec) of 100 nA for 10 min. After completing this protocol, the skin was sutured, rats were given analgesics (5 mg/kg Anafen), and the rats were returned to the animal facilities.

Twenty-four to 48 hr after FG injection, animals were anesthetized with pentobarbital (50 mg/kg) supplemented as needed with xylazine (5 mg/kg) for the surgery. The left facial nerve was cut, and the rat was placed in a stereotaxic apparatus. Throughout the experiment, the animal breathed freely, and body temperature was maintained at 37.5°C with a heating pad controlled thermostatically. Two stainless steel tubes (diameter, 1.5 mm; length, 15 mm; spacing, 10 mm) were fixed across the

surface of the skull by means of screws and acrylic cement. Trephine holes were drilled, and ear bars were removed. For the recording session, the rat's head was maintained in a stereotaxic position by means of a small U-shaped frame bearing adjustable pins inserted in the tube openings of the cemented device. The frame was secured to a large steel post so that whiskers on the left mystacial pad were freely accessible for stimulation. Before the start of the recordings, the nape of the neck was infiltrated with a long-lasting local anesthetic (1% Marcaine) to reduce animal discomfort. Local anesthesia produced a remarkably still preparation in which the electroencephalogram (recorded in two rats) displayed spindles and a dominance of 5–7 Hz activity. Animals remained motionless with occasional twitches of the right whiskers, indicating that they did not experience any discomfort, but they briskly reacted to a moderate pinch of the hind limbs. Together, these signs are indicative of a light anesthesia stage (stage III-2) (Friedberg et al., 1999). An additional dose of anesthetics (20 mg/kg ketamine) was given when small amplitude whisking movements were noticed.

Extracellular recordings were made with fine micropipettes (diameter, 0.5–1 μm) filled with K-acetate (0.5 M) and Neurobiotin (2%; Vector Laboratories, Burlingame, CA). Signals were amplified and bandpass filtered (100 Hz to 3 kHz) by conventional means. Analog signals were digitized at 20 kHz (Powerlab; AD Instruments, Castle Hill, Australia) and stored on hard disk. After completion of the stimulation protocol, neurons were stained juxtacellularly by the application of positive current pulses (2–8 nA; 200 msec duration; 50% duty cycle) for 5–10 min (Pinault, 1996). At the end of the experiments, rats were perfused under deep anesthesia with saline, followed by a fixative containing 4% paraformaldehyde and 0.5% glutaraldehyde in phosphate buffer (0.1 M; pH 7.4). Brains were removed, postfixed overnight in the same fixative, and cut coronally ($n = 25$) or horizontally ($n = 20$) at 70 μm with a vibratome.

In six additional experiments, coarser micropipettes (tip diameter, ~2 μm) were used for the simultaneous recording of pairs of VPM neurons. Units within a pair responded to the same principal whisker, and the directionality of responses was tested as described below.

Vibrissa stimulation and data analysis. A hand-held probe was used to identify cells that responded to the whisker, the barreloid of which had been labeled retrogradely with FG. Most cells responded strongly to one whisker (the principal whisker) and more weakly to one to three adjacent whiskers, whereas a minority (~10%) reacted robustly to the motion of four to eight whiskers. Latter units were principally encountered in the dorsalmost part of the VPM and were classified as multiwhisker-responsive cells. They were not considered in the present study, because in the first experiments the angular tuning preference of these units was found inconsistent across the stimulated vibrissas. Once a responsive unit had been isolated, the vibrissa was cut at 10 mm from the skin, and the tip was inserted into the groove of a beveled straw attached to a ceramic bimorph bender (Physik Instrumente, Karlsruhe, Germany). Care was taken to align the axis of the stimulator with that of the hair shaft. Before starting the stimulation protocol, we waited until the spontaneous activity became dominated by single spike discharges to avoid response magnitude to be biased by the presence of bursts. The potential impact of the bursty mode on angular tuning is unknown, but it has been clearly established that it can produce nonlinear enhancement of lemniscal inputs (Brecht and Sakmann, 2002; Castro-Alamancos, 2002). Ramp-and-hold waveforms (rise/fall times, 15 msec; total duration, 300 msec; amplitude, 1–2 mm) were used to deflect whiskers from their resting position in eight directions spanning 360° (e.g., in 45° increments relative to the horizontal alignment of the whisker rows). Stimuli were repeated 20 times, then the probe was rotated by 45°, and the sequence was repeated. At the end of the run, an additional sequence was performed at the starting direction to verify the stability of responses. Cells were included in the database if response magnitudes evoked by the first and last sequences (e.g., the same direction tested twice at ~10 min interval) did not differ at a 5% significance level (paired *t* test).

Spike events were compiled into peristimulus time histograms (PSTHs) of 20 responses with 1 msec bin width. For each deflection angle, the number of spikes evoked within a time window of 25 msec after stimulus onset was used to build polar plots of angular preference. When maximum response magnitudes were similar for two adjacent angles (two cells), the maximum magnitude was assigned midway between both directions. Although OFF responses also displayed clear directional sensitivity, we did not conduct quantitative analyses of OFF response tuning, because OFF response magnitudes in thalamic cells not only depend on the directional tuning of incoming fibers but also on postinhibitory rebound discharges (Kyriazi et al., 1994). Two measures of angular tuning preference were used to categorize cell responses: the maximum angle response and the resulting vector response. Because the latter measure is a weighted function of cell responsiveness to all directions, it is less likely to yield ambiguous results when response magnitude to the best angle differs little from that to adjacent angles. However, it was found that both measures were highly correlated ($R^2 = 0.87$; $p < 0.0001$) and yielded results of similar statistical significance. Thus, in the present study, we only describe the relationships between cell location and maximum angle response. To compare our data with those of previous studies (Simons and Carvell, 1989; Minnery et al., 2003), we calculated for each cell a tuning ratio, defined as the average ON response (all angles) divided by the ON response at the best angle. A directional tuning index was also computed for each neuron. Cells were categorized according to the number of deflection angles (0–7) that elicited a response that was statistically smaller than the maximum angle response (one-tailed *t* test; $p < 0.05$). Category 0 represents the least tuned cells, and category 7 represents the most.

In pair recordings, only units with an amplitude of at least three times the noise level were considered for analyses. Unit discrimination was performed with a time/amplitude window discriminator and also under visual supervision, because coincident spiking of both units after stimulus onset was common and could not be detected by the discriminator. First, a PSTH was constructed by discriminating only the larger unit; then, all sweeps were aligned, and the occurrence of the smaller unit within the first 25 msec after stimulus onset was detected visually. Counts were compiled manually into a separate PSTH, and the response magnitudes of both units were compared by means of polar plots.

Barreloid reconstruction and cell location. Barreloids and neurons were reconstructed from serial sections with the aid of a computer system (Neurolucida, version 5; Microbrightfield Inc., Colchester, VT). Arrays of retrogradely labeled cells were outlined by convex contours that were smoothed and connected to generate a solid picture of the barreloids. Each cell was assigned a location within its home barreloid using the following linear measures. The vertical distance between the cell body and the dorsal border of the barreloid (e.g., next to the VPM/posterior group border) was used as a measure of the dorsoventral location along the length of a barreloid (see Fig. 2*a*). The anteroposterior and mediolateral locations within the barreloid were determined with respect to the center of the home barreloid of the cell (crossing point of minor axis), positive values pointing forward and lateralward, and negative values pointing backward and medialward. All measurements were made after correction for shrinkage in the *z*-axis of the sections. The shrinkage factor was determined by computing the ratio of section thickness used for tissue sectioning to that measured on slides with the *z*-axis of the microscope stage. No correction was introduced for measurements along the *x*- and *y*-axes, because shrinkage along these dimensions was minimal (<10%) and did not modify the topographic relationship between barreloids and cell location.

Using the above-described coordinate system, cells were positioned in a model barreloid that had been reconstructed after the backfilling of barreloid D3. Because our sample consisted principally of D3-responsive cells, and because the length of the two other barreloids (C3 and D4) that contained labeled cells differ from that of barreloid D3 by ~100 μm [see also measurements made by Haidarliu and Ahissar (2001)], it was not found necessary to normalize cell position across our sample. The relationship between cell location and angular tuning preference was assessed by linear regression, cluster analysis (Ward method), and discriminant analysis.

Histochemistry and immunohistochemistry. After three washes in PBS (0.01 M; pH 7.4), brain sections were treated for 30 min with a solution of 50% ethanol plus 1% hydrogen peroxide. They were rinsed several times in PBS and preincubated for 1 hr in PBS with 3% normal goat serum and

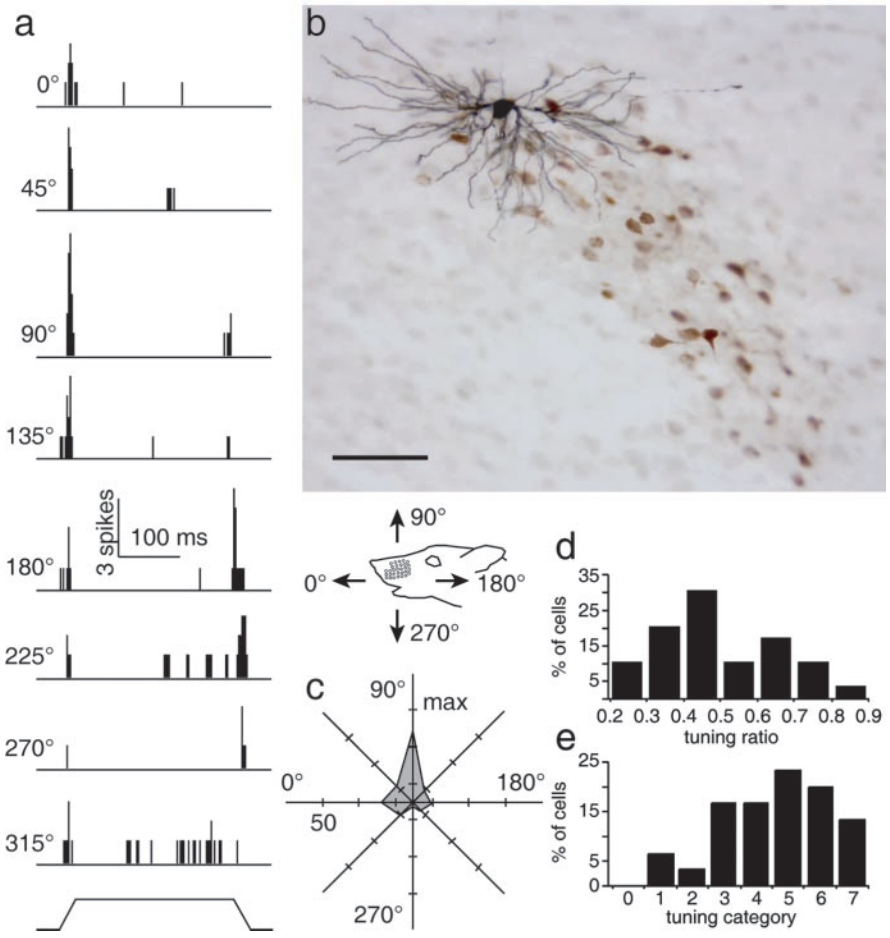

Figure 1. Combined determination of the angular tuning preference and location of relay cells within a barreloid. PSTHs were compiled from 20 responses to ramp-and-hold deflections of vibrissa D4 in eight different directions (*a*). Maximum ON responses were observed after upward deflection (polar plot in *c*). After the test, the cell was stained juxtacellularly with Neurobiotin, and a photomicrograph (*b*) shows its location in the dorsal part of barreloid D4, which had been prelabeled by the retrograde transport of FG. Scale bar, 100 μm. *d*, *e*, Distribution of tuning ratios and tuning indices, respectively, for the 30 VPM cells sampled in the present study.

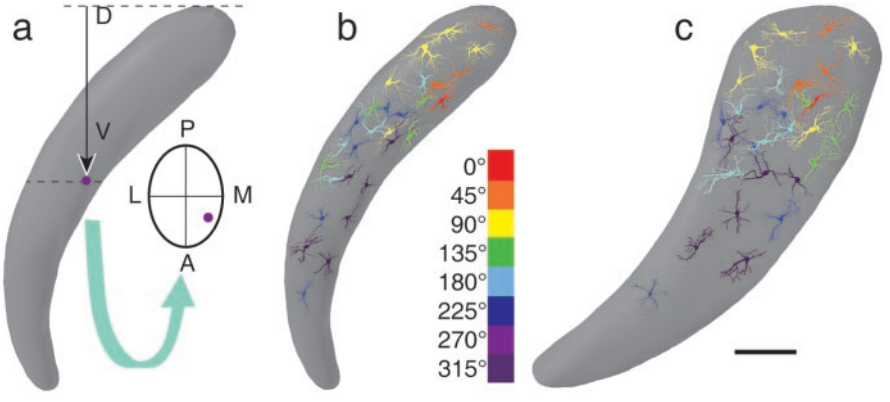

Figure 2. Relationship between angular tuning preference and cell location within a barreloid. The method used to measure cell location is shown in *a*. D, Dorsal; V, ventral; P, posterior; A, anterior; M, medial; L, lateral. The curved arrow points to a cross-section of the barreloid at the dotted line (see Materials and Methods for details). The color-coded display in *b* and *c* show how cells with different angular preferences distribute across the coronal and sagittal planes, respectively; only the somata and proximal dendrites are shown. Scale bar, 100 μm.

0.3% Triton-X. Then, they were incubated overnight in the same medium containing an anti-FG antiserum (1:8000; Chemicon, Temecula, CA). The antibody was revealed using a peroxidase-labeled secondary antibody (goat IgG; Chemicon) and DAB as a substrate (brown reaction product). Next, sections were processed for Neurobiotin histochemistry using an ABC kit (Vector Laboratories) and nickel-DAB (black reaction product). Finally, sections were mounted on gelatin-coated slides, dehydrated in alcohols, cleared in toluene, and coverslipped without counterstaining. Photomicrographs were taken with a Spot RT camera (Diagnostic Instruments Inc. Sterling Heights, MI) and imported in Photoshop 5.5 (Adobe Systems Inc., San Jose, CA) for contrast and brightness adjustments.

Results

The present study is based on combined anatomical and electrophysiological data obtained from 30 barreloid cells that, as a population, exhibited tuning ratios and angular tuning indices comparable with those reported in previous studies conducted in lightly sedated animals (Simons and Carvell, 1989; Hartings et al., 2000; Minnery et al., 2003). The mean tuning ratio ($\pm$ SD) was 0.49 $\pm$ 0.16, indicating a maximum angle ON response that was about double that of the average ON response (Fig. 1*d*). The majority of our sample (73%) had a tuning index of 4–7, revealing a strong tendency toward directional selectivity (Fig. 1*e*). Although we did not observe preferential tuning for any particular direction among our sample (Fig. 2), only one cell was found preferentially responsive to forward deflection (see Discussion).

Our sample consists of cells that best responded to deflection of the large caudal vibrissas (D3, $n = 23$; C3, $n = 5$; D4, $n = 2$). Figure 1 shows a representative example of a D4-responsive cell that best responded to upward vibrissa deflection and was located in the dorsal region of the labeled barreloid. Each cell so studied was assigned a location in a model barreloid using a three-dimensional coordinate system (see Materials and Methods) (Fig. 2*a*). The coronal and sagittal reconstructions of Figure 2, *b* and *c*, show how neurons with different angular preferences distributed across the dimensions of the model barreloid. One can note that cells best tuned to forward and upward directions are found principally in the dorsal sector of the barreloid, whereas those best activated by backward and downward whisker motion are located principally in the central and ventral sectors, respectively. Attempts to relate cell location to other direction parameters (tuning ratios, tuning indices) did not reveal any relationship (all $R^2 <$ 0.02), and we did not observe any obvious relationship between response directionality and cell morphology.

Although the color-coded distribution of Figure 2 presents pictorial evidence for the nonrandom location of cells with like

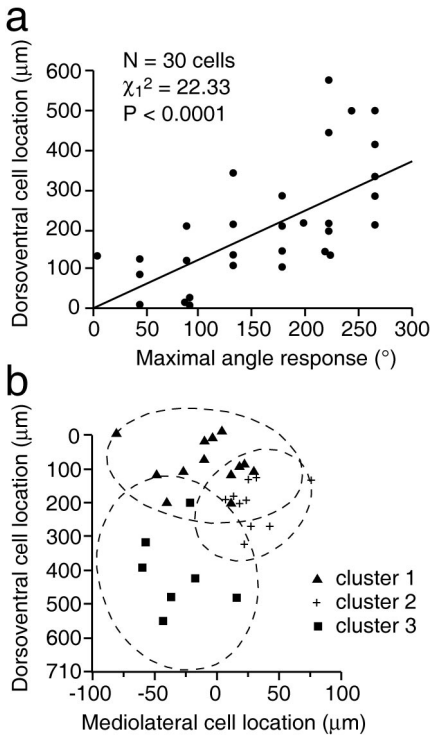

Figure 3. Scatterplots showing how cell location within a barreloid depends on the angular tuning of maximum responses. The plot in *a* shows the result of linear regression between angular tuning and dorsoventral location. The scatter diagram in *b* shows a visual display of cluster analysis. For numerical values of cellular aggregates, see Table 1.

Table 1. Mean and SE of the location measures and maximal angle responses for each cluster

	Cluster 1 ($n = 13$)	Cluster 2 ($n = 10$)	Cluster 3 ($n = 7$)
Location variables (μm)			
Mediolateral	−8.86 (8.93)	29.28 (6.02)	−31.23 (10.00)
Dorsoventral	95.51 (19.36)	212.70 (21.27)	416.28 (44.34)
Anteroposterior[a]	10.54 (26.31)	−5.19 (27.38)	10.58 (30.28)
Response (°)			
Maximal angle response	90 (13.48)	204.70 (11.84)	253.86 (8.10)
ANOVA			
Cluster aggregation	1–2	2–3	3–1
p values[b]	<0.0001	<0.0197	0.0001

[a]The anteroposterior measure is not used to cluster the cells.

[b]p values of the equality of maximal angle response mean between clusters.

Table 2. Number of observations classified into the four groups (quadrants) when the discriminant analysis used the three location variables

	Classified into quadrant				
	1	2	3	4	Total
From quadrant					
1	7	1	1	0	9
2	2	5	1	0	8
3	0	2	11	0	13
4	0	0	0	0	0
Total	9	8	13	0	30

angular preference, it does not provide a quantitative assessment of their sectorial clustering. When we used univariate regression analysis, it suggested that, taken individually, one measure of location was correlated with the maximum angle response (e.g., dorsoventral: Wald statistic $\chi_1^2 = 22.33$; $p < 0.0001$; Fig. 3*a*). Taken alone, the mediolateral location was not significantly related to the maximum angle response ($\chi_1^2 = 0.37$; $p = 0.5416$), and neither was the anteroposterior location ($\chi_1^2 = 0.39$; $p = 0.5337$). Also, when we used multiple regression, entering the three location measurements into the model, only the dorsoventral measure was highly and significantly related to the maximum response ($\chi_1^2 = 28.90$; $p < 0.0001$), but the mediolateral location became nearly significant ($\chi_1^2 = 3.04$; $p < 0.0811$). This bivariate model explains 50% of the variance of the maximum response. Thus, if taken alone, the mediolateral measure has no relationship with the maximum response ($\chi_1^2 = 0.37$; $p = 0.5416$), but when we add it to the dorsoventral measure, it is almost significant at the 5% level.

Statistical assessment of clustering

To further investigate the relationship between the location measures and maximum angle responses, we performed cluster analysis, which provides the advantage of using an approach that does not impose a linear relationship between location and response variables. Cluster analysis consists in regrouping cells, so that each cluster represents a class of homogeneous cells. The analysis was done in two ways. First, the three location measures and maximum response values were used to cluster the observations. The best discrimination was the three clusters one, according to the three clustering criteria (cubic clustering criterion, pseudo F, and pseudo t^2), and accounted for 50% of the variance. Second, the analysis used only the dorsoventral and mediolateral locations and maximum responses to cluster the observations, given that these two location variables were the most related to the maximum response in regression analysis. The best discrimination was again the three clusters one, which accounted for 65% of the variance. So, the most parsimonious model that best explains the variance is the one involving the dorsoventral and mediolateral measures. Accordingly, cells were regrouped into the following three clusters: $n = 13$ in cluster 1, $n = 10$ in cluster 2, $n = 7$ in cluster 3. One can refer to Figure 3*b* and Table 1 for the profile of each cluster. An ANOVA was used to test whether the three clusters have a significant variation in maximum response. The ANOVA suggests that the maximum response mean differs significantly from one cluster to another at the 5% level ($F = 44.5$; $p < 0.0001$).

Finally, discriminant analysis was used to determine whether angular preference could be predicted from the location variables. For that analysis, maximum response values were grouped into four quadrants (1–90°, 91–180°, 181–270°, and 271–360°). When the discriminant function was calculated with the three location variables, the total error count estimate was 0.2341 (Table 2). The percentage of agreement of 77% is significantly higher ($p < 0.0001$) than the one expected by chance (e.g., 35%). The corresponding measure of agreement that takes into account the rate of correct classification by chance is the κ coefficient, which yielded a value of 70% when a misclassification of a difference of two classes has twice the weight of a misclassification of a single class difference. Thus, together, regression, cluster, and discriminant analysis confirm in three different ways that the location of a cell within a barreloid relates to its angular tuning preference.

Pair recordings

The clustering of cells with like angular preference was assessed further by recording pairs of neighbor neurons responding to the same principal whisker. Figure 4 shows an example of two simul-

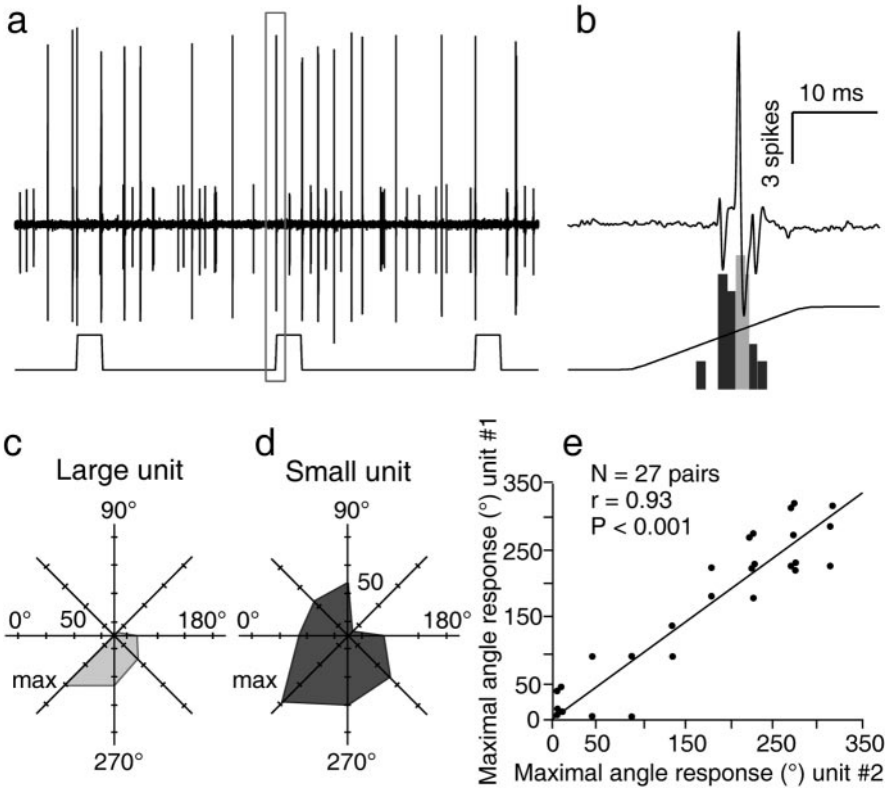

Figure 4. Correlation between the angular tuning preferences among pairs of neighboring cells. The two simultaneously recorded units in *a* were both maximally responsive to deflection in the forward/downward direction, as shown in the PSTH in *b* (top trace displays the framed segment in *a*) and in the polar plots in *c* and *d*. The plot in *e* shows the strong correlation found between the angular tuning preferences within 27 pairs of neurons.

taneously recorded D3-responsive units that were both maximally responsive to vibrissa displacements in the forward/downward direction (315°). A similar test was performed with 27 pairs of cells, and the graph of Figure 4 shows the strong relationship between angular preferences within each of these pairs ($r = 0.93$; $p < 0.0001$). The mean difference (±SD) in angular tuning within cell pairs was 30.00 ± 27.90°.

Discussion

The principal finding of the present study is that cells with like angular preference are clustered within the barreloids. Although clusters of differently tuned neurons partly overlap, they demonstrate a gradual shift of mean angular preference as one moves from the dorsal to the ventral region of a barreloid. This conclusion is supported by three different statistical tests, which indicates that barreloids contain a map of shifting angular preference that transposes along the length of a barreloid directional property imposed at the periphery by the circumferential distribution of receptors around the vibrissa follicles.

Methodological considerations

Although all statistical tests indicate a significant relationship between angular tuning preference and cell location, a number of factors may contribute to blur this relationship: (1) methodological factors; and (2) factors related to the intrinsic organization of the barreloids. First, our sample contains cells pertaining to different barreloids in different rats, so that similar linear distances along the dorsoventral axis do not necessarily coincide with the exact same locus across the barreloids. To a lesser degree, that distance is also sensitive to differences in the plane of tissue sectioning. It is difficult to estimate the amount of cell mislocation introduced by these factors, but they likely contribute to intermingle cells with different angular preference. This is, indeed, suggested by the strong correlation observed in pair recordings that did not rely on any spatial measurements. Second, the proximal dendrites of individual cells on which lemniscal axons terminate radiate out from the cell bodies over a sizeable distance (e.g., ~40 μm) (Spacek and Lieberman, 1974; Varga et al., 2002), and the numerous fiber bundles that traverse the VPM may force cell dispersion. Thus, two cells 80 μm apart (note: barreloids are ~100 μm wide in the coronal plane) with interdigitating proximal dentritic trees could receive inputs from the same lemniscal fibers and, thus, demonstrate closely related angular preferences. Developmental factors likely contribute to spread cell clusters; the initial layout of the cellular components in the barreloids gets transformed during development. It has been shown that lemniscal afferents are present in VPM at birth (Belford and Killackey, 1979; Ivy and Killackey, 1982; Erzurumlu and Killackey, 1983) and that a clear whisker-related pattern appears in the ventrobasal complex of the thalamus between postnatal days 2 and 4 (Belford and Killackey, 1980). During the first postnatal weeks, the thalamus expands, so that barreloids double in length and acquire a curved shape (Haidarliu and Ahissar, 2001). Thus, growth-associated transformations may produce cell translation and a certain amount of rotation and twisting of the barreloids, which could contribute to modify the initial position of the elements.

Although many units responded to forward whisker motion, few were found preferentially responsive to that direction. We have no reason to believe that this scarcity results from a sampling error related to our stimulation protocol. In contrast, we cannot exclude the possibility that facial nerve cut may have reduced primary afferent responsiveness to forward deflection, thus introducing a bias in the expression of direction tuning. Because no previous study can be used as a comparative basis, additional experiments will be required to assess this point.

Cells that responded robustly to multiple whiskers were not considered in the present study because their direction preference was found inconsistent across the stimulated whiskers. These units were found principally in the dorsalmost sector of the barreloids among cells preferentially responsive to rostral and dorsal directions. We did not keep records of all units encountered in our experiments, but on the basis of data obtained in separate series of experiments, multiwhisker cells account for ~10% of the recorded units. Previous tract tracing studies have shown that the dorsalmost sector of the barreloids is innervated selectively by a small proportion (4%) of large multiwhisker PR5 units (Veinante and Deschênes, 1999) and by a subgroup of reticular thalamic cells (Désilets-Roy et al., 2002). The question of whether these units are components of a parallel channel of vibrissal information remains, as yet, an unresolved issue.

Angular preference is not the sole parameter that characterizes receptive field properties in the vibrissa system. Cell responses are also modulated by the amplitude and velocity of displacements, but no study has yet demonstrated an influence of these factors on angular tuning preference. Thus, although different amplitude and velocity thresholds may define parallel channels of information in the system (Shipley, 1974; Shoykhet et al., 2000), it seems unlikely that the map of angular preference disclosed in the present study would have been modified significantly by deflecting whiskers over wider ranges of amplitude or velocity.

A more perplexing issue is whether the deflection of isolated vibrissas represents an optimal stimulation protocol for assessing angular preference. Nonlinear enhancement of response magnitudes have already been reported in the VPM after simultaneous stimulation of adjacent whiskers (Ghazanfar and Nicolelis, 1997), but the critical point here is whether this enhancement might introduce significant changes in angular preference. Although we cannot exclude this possibility, our results, nevertheless, show that principal whisker deflection alone is a sufficient condition to disclose an orderly map of angular preference. That map could possibly be sharpened by multiwhisker deflection, but it would be a remarkable finding if its topography could be dynamically modified by the spatiotemporal patterns of sensory stimuli.

Anatomic substrate for an angular preference map

On the basis of the neuronal density in the rat VPM, it was estimated that barreloids representing the large caudal vibrissas contain ~200 relay cells (Land et al., 1995; Varga et al., 2002). Given the size of corresponding PR5 barrelettes (diameter, ~55 μm; length, ~1.2 mm) (Henderson and Jacquin, 1995), one can already suspect that they contain an approximate equal number of neurons. Counts obtained after confocal reconstructions of NeuN immunostained sections yield a similar figure for the number of small-sized neurons in PR5 barrelettes (e.g., 160–200 cells; our unpublished observations). Taking into account the small terminal field of PR5 axons in thalamic barreloids (e.g., ~80 μm) (Williams et al., 1994; Veinante and Deschênes, 1999), a one-to-one numerical relationship implies a low convergence ratio in the barrelette-to-barreloid connections. Intracellular studies, indeed, indicate that individual barreloid neurons receive synaptic inputs from an average of one to three medial lemniscal fibers (Castro-Alamancos, 2002; Deschênes et al., 2003). Because PR5 and VPM cells exhibit similar tuning ratios and similar tuning indices (Minnery et al., 2003), the convergence of lemniscal axons onto barreloid cells ought to be related, at least in part, to the directional properties of incoming fibers. Again, because PR5 axons form small-sized terminal fields, it follows that neighbor cells within a barreloid should exhibit closely related angular preferences. Thus, the strong correlation observed in the present study between the angular tuning of neighbor cells provides direct evidence that cells with like angular preference are clustered within the barreloids. This conclusion is also supported by the study of Temereanca and Simons (2003) that actually anticipated the present results, and in which it was shown that the amplitude of whisker-evoked field potentials recorded at different depths within a barreloid depended on the direction of whisker displacements.

Functional maps in barrel cortex

The presence of an angular preference map in the barreloids raises the issue of whether a similar map also exists in cortical barrels. It has been shown that whisker-evoked responses in layer 4 stellate cells are direction sensitive (Simons and Carvell, 1989). Assuming 250 neurons per barreloid, Bruno and Simons (2002) estimated that an excitatory stellate cell was likely to be influenced, on average, by 90 thalamocortical neurons, which implies that individual barrel cells receive inputs from differently tuned thalamic neurons. Although we still have limited information on how the terminal field of individual thalamocortical fibers distributes in a barrel, it seems possible that barreloid cells with different angular preference form spatially distinct gradients of terminations inside the barrels. The synaptic efficacy of the thalamic inputs would then depend on the location of the cell within the terminal fields. Such a pattern of connections could explain why, despite convergence, barrel cells remain tuned to the angle of deflection, but it does not explain why no angular preference map has yet been disclosed in the cortex. One possibility could be that barrels contain a map of higher integration level, the disclosure of which requires a different stimulation protocol. As far as the visual system can be used as a model, it is worth noting that cells in area 17 are poorly responsive to the circular light spots to which geniculate cells strongly react. Because barrel cells have extensive subthreshold receptive fields (Moore and Nelson, 1998), because inhibitory processes are prevalent and powerful in the barrels (Simons and Carvell, 1989; Armstrong-James et al., 1993; Kyriazi et al., 1996; Brumberg et al., 1996), and because inhibitory interneurones strongly respond to the deflections of several whiskers (Simons and Carvell, 1989; Brumberg et al., 1996), it seems plausible, as suggested previously (Moore et al., 1999), that a multiwhisker stimulation protocol would be better appropriate to disclose a direction-dependent functional map in the barrels.

References

Armstrong-James M, Welker E, Callahan CA (1993) The contribution of NMDA and non-NMDA receptors to fast and slow transmission of sensory information in the rat SI barrel cortex. J Neurosci 13:2149–2160.

Belford GR, Killackey HP (1979) The development of vibrissae representation in subcortical trigeminal centers of the neonatal rat. J Comp Neurol 188:63–74.

Belford GR, Killackey HP (1980) The sensitive period in the development of the trigeminal system of the neonatal rat. J Comp Neurol 193:335–350.

Brecht M, Sakmann B (2002) Whisker maps of neuronal subclasses of the rat ventral posterior medial thalamus, identified by whole-cell voltage recording and morphological reconstruction. J Physiol (Lond) 538:495–515.

Brumberg JC, Pinto D, Simons DJ (1996) Spatial gradients and inhibitory summation in the rat whisker barrel system. J Neurophysiol 76:130–140.

Bruno RM, Simons DJ (2002) Feedforward mechanisms of excitatory and inhibitory cortical receptive fields. J Neurosci 22:10966–10975.

Castro-Alamancos MA (2002) Properties of primary sensory (lemniscal) synapses in the ventrobasal thalamus and the relay of high-frequency sensory inputs. J Neurophysiol 87:946–953.

Deschênes M, Timofeeva E, Lavallée P (2003) The relay of high-frequency sensory signals in the whisker-to-barreloid pathway. J Neurosci 23:6778–6787.

Désîlets-Roy B, Varga C, Lavallée P, Deschênes M (2002) Substrate for cross-talk inhibition between thalamic barreloids. J Neurosci 22:RC218.

Ebara S, Kumamoto K, Matsuura T, Mazurkiewicz JE, Rice FL (2002) Similarities and differences in the innervation of mystacial vibrissal follicle–sinus complexes in the rat and cat: a confocal microscopic study. J Comp Neurol 449:103–119.

Erzurumlu RS, Killackey HP (1983) Development of order in the rat trigeminal system. J Comp Neurol 213:365–380.

Friedberg MH, Lee SM, Ebner FF (1999) Modulation of receptive field properties of thalamic somatosensory neurons by the depth of anesthesia. J Neurophysiol 81:2243–2252.

Ghazanfar AA, Nicolelis MAL (1997) Nonlinear processing of tactile information by thalamocortical ensembles. J Neurophysiol 78:506–510.

Gibson JM, Welker WI (1983) Quantitative studies of stimulus coding in

first-order vibrissa afferents of rats. 1. Receptive field properties and threshold distributions. Somatosens Res 1:51–67.
Haidarliu S, Ahissar E (2001) Size gradients of barreloids in the rat thalamus. J Comp Neurol 429:372–387.
Hartings JA, Temereanca S, Simons DJ (2000) High responsiveness and direction sensitivity of neurons in the rat thalamic reticular nucleus to vibrissa deflections. J Neurophysiol 83:2791–2801.
Henderson TA, Jacquin MF (1995) What makes subcortical barrels? In: Cerebral cortex, Vol 12, The barrel cortex of rodents (Jones EG, Diamond IT, eds), pp 123–187. New York: Plenum.
Ito M (1988) Response properties and topography of vibrissa-sensitive VPM neurons in the rat. J Neurophysiol 60:1181–1197.
Ivy GO, Killackey HP (1982) Ephemeral cellular segmentation in the thalamus of the neonatal rat. Dev Brain Res 2:1–17.
Knudsen EI, du Lac S, Esterly SD (1987) Computational maps in the brain. Annu Rev Neurosci 10:41–65.
Kyriazi HT, Carvell GE, Simons DJ (1994) OFF response transformations in the whisker/barrel system. J Neurophysiol 72:392–401.
Kyriazi HT, Carvell GE, Brumberg JC, Simons DJ (1996) Quantitative effects of GABA and bicuculline methiodide on receptive field properties of neurons in real and simulated whisker barrels. J Neurophysiol 75:547–560.
Land PW, Buffer SA, Yaskosky DJ (1995) Barreloids in adult rat thalamus: three-dimensional architecture and relationship to somatosensory cortical barrels. J Comp Neurol 355:573–588.
Lee SM, Friedberg MH, Ebner FF (1994) The role of GABA-mediated inhibition in the rat ventral posterior medial thalamus. I. Assessment of receptive field changes following thalamic reticular nucleus lesions. J Neurophysiol 71:1702–1715.
Lichtenstein SH, Carvell CA, Simons DJ (1990) Responses of rat trigeminal ganglion neurons to movements of vibrissae in different directions. Somatosens Motor Res 7:47–75.
Minnery BS, Simons DJ (2003) Response properties of whisker-associated trigeminothalamic neurons in rat nucleus principalis. J Neurophysiol 89:40–56.
Minnery BS, Bruno RM, Simons DJ (2003) Response transformation and receptive field synthesis in the lemniscal trigeminothalamic circuit. J Neurophysiol 90:1556–1570.
Moore CI, Nelson SB (1998) Spatio-temporal subthreshold receptive fields in the vibrissa representation of rat primary somatosensory cortex. J Neurophysiol 80:2882–2892.
Moore CI, Nelson SB, Sur M (1999) Dynamics of neuronal processing in rat somatosensory cortex. Trends Neurosci 22:513–520.
Pinault D (1996) A novel single-cell staining procedure performed in vivo under electrophysiological control: morpho-functional features of juxtacellularly labeled thalamic cells and other central neurons with biocytin or Neurobiotin. J Neurosci Methods 65:113–136.
Shipley MT (1974) Response characteristics of single units in the rat's trigeminal nuclei to vibrissa displacements. J Neurophysiol 37:73–90.
Shoykhet M, Doherty D, Simons DJ (2000) Coding of deflection velocity and amplitude by whisker primary afferent neurons: implications for higher level processing. Somatosens Motor Res 17:171–180.
Simons DJ, Carvell GE (1989) Thalamocortical response transformation in the rat vibrissa/barrel system. J Neurophysiol 61:311–330.
Spacek J, Lieberman AR (1974) Ultrastructure and three-dimensional organization of synaptic glomeruli in rat somatosensory thalamus. J Anat 117:487–516.
Temereanca S, Simons DJ (2003) Local field potentials and the encoding of whisker deflections by population firing synchrony in thalamic barreloids. J Neurophysiol 89:2137–2145.
Van der Loos H (1976) Barreloids in the mouse somatosensory thalamus. Neurosci Lett 2:1–6.
Varga C, Sik A, Lavallée P, Deschênes M (2002) Dendroarchitecture of relay cells in thalamic barreloids: a substrate for cross-whisker modulation. J Neurosci 22:6186–6194.
Veinante P, Deschênes M (1999) Single- and multi-whisker channels in the ascending projections from the principal trigeminal nucleus in the rat. J Neurosci 19:5085–5095.
Williams MN, Zahm DS, Jacquin MF (1994) Differential foci and synaptic organization of the principal and spinal projections to the thalamus in rats. Eur J Neurosci 6:429–453.
Woolsey TA, Van der Loos H (1970) The structural organization of layer IV in the somatosensory region (S1) of mouse cerebral cortex. The description of a cortical field composed of discrete cytoarchitectonic units. Brain Res 17:205–242.
Zucker E, Welker WL (1969) Coding of somatic sensory input by vibrissae neurons in the rat's trigeminal ganglion. Brain Res 12:138–156.